Induced Gamma-band Activity Elicited by Visual Representation of Unattended Objects

Jasna Martinovic[1,2], Thomas Gruber[1], Kathrin Ohla[1], and Matthias M. Müller[1]

Abstract

■ Object recognition is achieved through neural mechanisms reliant on the activity of distributed neural assemblies that are thought to be coordinated by synchronous firing in the gamma-band range (>20 Hz). An outstanding question focuses on the extent to which the role of gamma oscillations in object recognition is dependent on attention. Attentional mechanisms determine the allocation of perceptual resources to objects in complex scenes biasing the outcome of their mutual competitive interactions. Would object-related enhancements in gamma activity also occur for unattended objects when perceptual resources are traded off to the processing of concurrent visual material? The present electroencephalogram study investigated event-related potentials and evoked (time- and phase-locked) and induced (non-time- and phase-locked to stimulus onset) gamma-band activity (GBA) using a visual discrimination task of low or high perceptual load at fixation. The task was performed while task-irrelevant familiar or unfamiliar objects coappeared in the surrounding central area. Attentional focus was kept at fixation by varying perceptual load between trials; in such conditions, only holistic object processing or low-level perceptual processing, requiring little or no attention, are thought to occur. Although evoked GBA remained unmodulated, induced GBA enhancements, specific to familiar object presentations, were observed, thus providing evidence for cortical visual representation of unattended objects. In addition, the effect was mostly driven by object-specific activity under low load, implying that, in cluttered or complex scenes, attentional selection likely plays a more significant role in object representation. ■

INTRODUCTION

Various attentional models have attempted to describe mechanisms through which stimuli, based on their task relevance, are either ignored or selected for further processing (e.g., Duncan, 1980; Treisman, 1969). Spatial, feature-based, and object-based attention are thought to rely differentially on a set of rapidly functioning neural mechanisms that allow enhancement of attended and suppression of unattended information (Reynolds & Chelazzi, 2004). Selective attention is essential for efficient processing as sensory information constantly competes for the limited set of available resources (Desimone, 1998). To address this, Lavie (1995) proposed a model of attentional processing that takes into account the amount of perceptual information (referred to as ''perceptual load'') that the visual system has in order to perform accurate discriminations. Perceptual load is enhanced when the number of items to be processed is increased, or when the task is altered to require discrimination between highly similar features or multiple feature conjunctions. Depending on the amount of load, attentional mechanisms distribute perceptual resources across the rest of the scene to ensure efficient processing. One such mechanism reduces the processing of irrelevant information (referred to as ''distractors'') when the perceptual load becomes high; another automatically allocates to other elements of a scene, when the perceptual load is low, even if they are task-irrelevant (Lavie, 1995).

A selective attention mechanism that controls the allocation of perceptual resources across visual scenes on the basis of stimulus relevance and task demands is very important for visual object representation. Attention is known to play an essential role in guiding the selection and processing of objects in everyday vision. Relevant objects are given processing priority and placed within the attentional spotlight (Schroeder, Mehta, & Foxe, 2001)—they are foveated, recognized, and acted upon. However, to what level are unattended objects processed? Visual scenes contain large numbers of objects with varying amounts of clutter and mutual occlusion; these objects are constantly competing for processing resources. Their relevance for the individual's present motivational state influences the outcome of the competition as relevant objects are given processing priority through attentional selection. But which representation type, if any, is formed for unattended objects?

It is generally considered that certain processing streams within the object recognition system do not require attention, thereby allowing for implicit registration

[1]Universität Leipzig, Germany, [2]University of Liverpool, UK

of unattended objects up to a certain level of representation (for overviews, see Thoma, Hummel, & Davidoff, 2004; Murray & Jones, 2002). This level is mostly assumed to contain lower-level representations of visual features within the image and their conjunctions (e.g., color or shape) and to exclude higher-level semantic-based information. Although certain studies found that even unattended objects were habitually being processed up to the semantic level (e.g., Altmann, Grodd, Kourtzi, Bülthoff, & Karnath, 2005; Pins, Meyer, Foucher, Humphreys, & Boucart, 2004), other studies which explicitly controlled attention indicated there is very little or no identification without attention (Lachter, Forster, & Ruthruff, 2004). A recent behavioral study by Thoma et al. (2004) demonstrated that visual representations of ignored objects are holistic in nature, whereas those of attended objects are analytic. In the hybrid model of object recognition, these two types of visual representations occur in parallel and make contact with object memory independently; although only analytic representations contain explicitly delineated relations among an object's parts. Holistic representations do not define these relations explicitly or independently of the parts but instead represent them within a coordinate system that refers to one particular view of the object (Hummel & Stankiewicz, 1996).

Support for the hybrid model shows that the level of representation depends on the allocation of attention. A behavioral study by Murray and Jones (2002) adopted Lavie's (1995) model of perceptual load in order to systematically examine the relation between perceptual mechanisms of attentional selection and processing of object representations. A task was used in which local form information, embedded within a task-irrelevant global familiar object-shape, had to be matched in orientation between a reference and a target/distractor display. This local form information could either be of low or high perceptual load which, when randomly intermixed between trials, avoided strategic biases in attentional deployment. With attention constrained to the local form information by top–down influences, no evidence of semantic processing of surrounding object-shapes was found under low or high load. Lower-level presemantic processing of surrounding object-shapes still took place, however, as identical distractors seemed to be processed more favorably, presumably due to requiring little or no attention.

Visuospatial attentional selection and the deployment of perceptual resources have also been examined neuroscientifically. Recent studies have examined the role of peripherally presented perceptual load in determining the extent of neural processing of simple visual information. Handy and Mangun (2000) looked at the role of load using event-related potentials (ERPs) and obtained attentional modulations of P1 and N1 components. They suggested this reflected early changes in the magnitude of spatial-selective processing in extrastriate visual areas, which increased with higher load. A related blocked design study by Handy, Soltani, and Mangun (2001) observed a decrease for distractors presented under high foveal load occurring at the level of P1, N1, and N2, indicating that perceptual load did affect the early stages of processing of simple task-irrelevant information. In a recent functional magnetic resonance imaging (fMRI) study, Schwartz et al. (2005) found that purely top–down increases in attentional load at fixation decreased responses to peripheral distractors at the level of the early visual cortex. The effect was larger for higher-level visual areas, suggesting attentional surround-suppression. High load, therefore, impacts on the neurophysiological markers of early visual processing by reducing responses to simple information in the periphery.

However, the question remains—what markers would be affected by complex visual information (i.e., objects) presented foveally under different types of perceptual load? Foveally presented items have preferential access to attention and therefore interfere more with the processing of task-relevant information (Beck & Lavie, 2005). The challenges posed by natural scenes in everyday life involve mutual occlusion of foveated objects amid varying degrees of background clutter. How does the brain manage to code each of these objects in a unified way? It has been suggested that neural mechanisms subserving object processing rely on the activity of distributed neural assemblies. This activity is thought to be coordinated by synchronous firing in the gamma-band range (>20 Hz). Such event-related gamma-band activity (GBA) can either be evoked (time- and phase-locked to stimulus onset) or induced (non-time- and phase-locked). Evoked GBA is generally focused in the lower gamma-band frequency ranges (30–40 Hz) and has a stable latency of approximately 100 msec; it is modulated by task complexity (Senkowski & Herrmann, 2002; for an opposite finding, see Posada, Hugues, Franck, Vianin, & Kilner, 2003) and feature-selective processing demands (Busch, Schadow, Fruend, & Herrmann, 2006) and reflects an early stream of sensory processing. Induced GBA shows greater variability in frequency (30–90 Hz) and usually peaks at approximately 250 msec, with the peak latency related to the time point of object recognition (Martinovic, Gruber, & Müller, 2007). Significant levels of induced GBA are elicited in studies that require identification of foveally presented familiar objects; it is likely that such induced GBA reflects a later stream of representational processing connected to visual memory processes (Gruber & Müller, 2005; Gruber, Malinowski, & Müller, 2004). Induced GBA is therefore highly relevant for object recognition studies.

The extent to which integrative oscillatory activity underlying visual object representation is attention-dependent has previously been researched using induced gamma-band responses as a measure of perceptual processing. There is some evidence supporting both the role of automatic, gestalt-like processes as well as the role of

perceptual attentional mechanisms (Müller & Gruber, 2001; Müller, Gruber, & Keil, 2000). Thus, it is still an open question if attention is a necessary prerequisite for object-related enhancements in induced GBA. What happens with induced GBA when objects are unattended? Moreover, would GBA amplitude depend on the perceptual load, with highly taxing visual discriminations engaging more perceptual resources away from the task-irrelevant objects? Although induced GBA under conditions of different perceptual load has yet to be investigated, if it is a specific marker of integratory processes in object identification, its amplitude should depend on the functioning of perceptual mechanisms of attentional selection.

The present electroencephalogram (EEG) study was conducted to provide answers to these outstanding questions: (1) Do induced GBA enhancements specific for object processing also occur for unattended objects? and (2) Is their amplitude influenced by differential task demands introduced through changes in the perceptual load? ERPs and evoked and induced GBA were investigated using a visual matching task of low or high perceptual load at fixation that was attended while task-irrelevant familiar or unfamiliar objects coappeared in the surrounding central area. The aim was to examine how much neural processing of surrounding familiar objects occurred when attention was directed to complex local form information. A further aim was to examine whether this processing differs when perceptual load of task-relevant information was changed from low to high, thereby influencing the extent of the automatic reallocation of residual resources to spatially coexistent distractors.

Based on previous findings on effects of stimulus size on both types of GBA (Busch, Debener, Kranczioch, Engel, & Herrmann, 2004), the small local form stimuli should elicit none or very low event-related GBA (both evoked and induced). This assumption was first tested in Experiment 1 by employing only the local form stimuli of low and high load without the surrounding distractors. This acted as a control for Experiment 2, which tested the hypothesized effects of distractors, either familiar or unfamiliar objects, under low and high perceptual load on ERPs, evoked and induced GBA. Induced GBA is elicited by foveal presentations of familiar but not unfamiliar words and objects (Fiebach, Gruber, & Supp, 2005; Gruber & Müller, 2005). Therefore, differential activations between familiar and unfamiliar objects were expected to be significant under low load due to the automatic reallocation of leftover resources to salient familiar stimuli and their representational processing. For high load, it was expected that familiar objects would not be able to trigger significant increases in induced GBA in relation to unfamiliar objects, as perceptual capacities would be exhausted by the demanding high load task at fixation (Lavie, Hirst, de Fockert, & Viding, 2004). Evoked GBA has also been modulated by object familiarity in a few studies (Fründ, Busch, Schadow, Gruber, Körner, & Herrmann, 2008; Morup, Hansen, Herrmann, Parnas, & Arnfred, 2006; Herrmann, Lenz, Junge, Busch, & Maess, 2004). Still, its object specificity is disputed because many more studies have failed to find an effect of object familiarity (Busch, Herrmann, Müller, Lenz, & Gruber, 2006; Gruber, Trujillo-Barreto, Giabbiconi, Valdes-Sosa, & Müller, 2006; Fiebach et al., 2005; Gruber & Müller, 2005; Tallon-Baudry, Bertrand, Delpuech, & Pernier, 1996). Robust previous findings indicate that evoked GBA is highly responsive to both bottom–up and top–down driven feature processing (e.g., Busch, Schadow, et al., 2006), with the assumption being that it is a necessary prerequisite for significant increases in induced GBA (Herrmann, Munk, & Engel, 2004). It was therefore hypothesized that evoked GBA would be elicited but that it would dissociate from induced GBA, being preferentially modulated by task demands.

In order to complement the findings on event-related GBA, ERPs were also examined focusing on the following components: early components P1 and N1, and late components L1 and L2. Previous studies have found characteristic modulations of late components by stimulus familiarity, with unfamiliar stimuli eliciting a more negative L1 and a more positive L2 (Gruber & Müller, 2005; Rugg, Soardi, & Doyle, 1995). As previously mentioned, Handy et al. (2001) observed more negativity for distractors under high load, occurring at the level of P1, N1, and N2. These authors speculated, however, that the P1 effect should be eliminated if load is subjected to trial-by-trial variations, as the attentional focus in these circumstances remains steady across load conditions. Because the allocation of attention was supposed to be equal at trial onset, due to unpredictability of both load and distractor type, it was expected that the early effects of load on P1 and N1 would not be observed. Effects of load could still occur at later processing stages so it was expected that these differences might be observed on the late components L1 and L2.

EXPERIMENT 1

In the control experiment, the central local form stimuli were piloted without any surround to verify the presence of behavioral effects of perceptual load and also to determine the optimal display times that would ensure desirable pacing for Experiment 2. EEG data were collected in order to establish that small foveal stimuli would not, by themselves, elicit significant enhancements in evoked or induced GBA. Because only familiar objects elicit significant increases in induced GBA (Gruber & Müller, 2005), this allows clear conclusions to be drawn about the interaction between object familiarity and perceptual load, which were to be examined in the main experiment.

Methods

Participants

Fourteen participants took part. Two had to be removed due to a technical error during EEG recording. Twelve participants (2 men) remained in the sample, aged 19 to 26 years (mean age = 22.5 years). They were all healthy, right-handed university students and received class credit or a small honorarium for participation. Participants reported normal or corrected-to-normal vision. Individual written informed consent was obtained and the study conformed to the Code of Ethics of the World Medical Association.

Materials and Procedure

In the center of the screen, an image was presented that contained three yellow boxes organized in a triangular fashion around a red fixation cross (see Figure 1). Participants were instructed to match the content of the upper box with the content of one of the two boxes below. The index and middle fingers of one hand were placed on the two side-by-side buttons and participants were told to press the button that corresponded to the side of the box with the correct match.

Based on Murray and Jones (2002), tasks differing in perceptual load were created. One hundred ninety-two stimuli, which included the original Murray and Jones (2002) set, were presented in a randomized order, different for each of the participants. In the low perceptual load condition, the upper and both of the lower two boxes contained line forms and the participant had to match the content of the upper box to the lower box that contained exactly the same form. In the high load condition, the lower boxes contained letters and participants had to match the line form from the upper box with the letter that fully contained such a line form within its shape. Participants were instructed to do this as quickly and as accurately as they could.

Participants first performed a practice block of 48 trials (24 per load level) that contained a subset of stimuli that were not used in the experiment itself. The practice was repeated until the participants reached a criterion of 80% correct.

The experiment itself consisted of four blocks, with each block lasting approximately 2 min and containing 48 trials. Each trial consisted of a variable 500–800 msec baseline period during which a red fixation cross ($0.2^\circ \times 0.2^\circ$) was presented. This was followed by a stimulus picture that was displayed for 600 msec. The picture was then replaced by the fixation cross, which remained on the screen for a period of 650 msec.

Stimuli ($1^\circ \times 1^\circ$) were shown on a white background and were presented centrally on a 19-in. computer screen, with a 70-Hz refresh rate, that was positioned 1 meter in front of the participant in a dimly lit soundproof testing chamber. Stimulus onset was synchronized to the vertical retrace of the monitor. The presentation and timing of the experiment were controlled using a MATLAB Toolbox, allowing precise visual presentation and response-recording timings (Cogent; www.vislab.ucl.ac.uk/Cogent/; The Mathworks, Natick, MA).

Halfway through the experiment, participants were asked to change the responding hand. Participants were instructed to minimize eye movements and blinking during the display of a stimulus or the fixation cross.

EEG Recording

EEG was recorded continuously from 128 locations using active Ag–AgCl electrodes (BioSemi Active-Two amplifier system) placed in an elastic cap, referenced to an additional active electrode (CMS = Common Mode Sense; with ground in additional electrode DRL = Driven Right Leg)

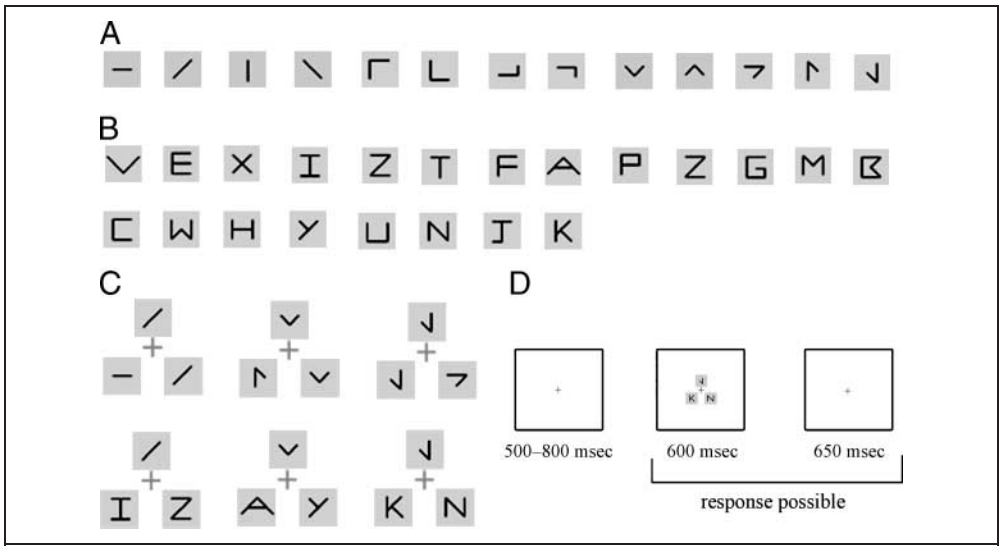

Figure 1. Examples of stimuli. (A) Low load items; (B) high load items; (C) low and high load items organized around a fixation cross so that the upper position is taken by the line form that is to be matched with one of the two line forms in the lower boxes (lines for low load, letters for high load); (D) trial outlook.

during recording. EEG signal was sampled at a rate of 512 Hz. Horizontal and vertical electrooculograms were recorded in order to exclude trials with blinks and significant eye movements. EEG was segmented into epochs starting 500 msec prior and lasting 1500 msec following picture onset. EEG data processing was performed using the EEGLAB toolbox (Delorme & Makeig, 2004), combined with self-written procedures running under Matlab (The Mathworks). Artifact correction was performed by means of ''statistical correction of artifacts in dense array studies'' (SCADS; Junghoefer, Elbert, Tucker, & Braun, 2000). This procedure is widely accepted in the field and has been applied and described in several publications (e.g., Müller & Keil, 2004; Gruber, Müller, Keil, & Elbert, 1999). The average rejection rate was 32.6%, resulting in approximately 57 remaining trials per condition on average. Further analyses were performed using the average reference.

Behavioral Data Analysis

RTs between 250 and 1250 msec (the maximum time allowed for responses) after stimulus onset on trials with correct responses were taken into further analysis. Mean RTs and error rates were computed for each participant. Differences in error rates and response speed between low and high perceptual load were analyzed using paired t tests.

Event-related Potentials Analysis

A 25-Hz low-pass filter was applied to the data before all ERP analyses.

Two ERP components were assessed: P1 and N1. For each component, regional means (shown in Figure 2; see Results) were assigned based on which electrodes exhibited maximal activity when data were collapsed across conditions. Average amplitudes across the electrodes at these sites in their respective time windows (80–120 msec for the P1, 130–190 msec for the N1) were then computed and the mean amplitude during the period 100 msec prior to stimulus onset (baseline) was subtracted. Mean latencies were not analyzed as there were no hypotheses concerning them. Differences in amplitude between low and high perceptual load were analyzed using paired t tests.

Analysis of Evoked and Induced Spectral Changes

Oscillatory activity was analyzed according to the standard procedure employed in a multitude of preceding studies (e.g., Gruber & Müller, 2005; Gruber et al., 2004). In brief, spectral changes in oscillatory activity were analyzed by means of Morlet wavelet analysis (Bertrand & Pantev, 1994), which provides a good compromise between time and frequency resolution (Tallon-Baudry & Bertrand, 1999). This method gives a time-varying magnitude of the signal in each frequency band leading to a time-by-frequency representation of the signal and is described in-depth, together with suggested parameter definitions that allow for a good time and frequency resolution in the gamma frequency range, in previous studies (e.g., Gruber & Müller, 2005). In order to achieve good time and frequency resolution in the gamma frequency range, the wavelet family was defined by a constant $m = f_0/\sigma_f = 7$, with f_0 ranging from 2.5 to 100 Hz in 0.5-Hz steps. These data were subsequently reduced to form 2.5-Hz-wide wavelets. Time-varying energy in a given frequency band was calculated for each epoch, this being the absolute value of the convolution of the signal with the wavelet for each complex spectrum.

Preliminary electrode sites used for time-by-frequency plots (TF plots) and further peak amplitude analyses were selected on the basis of previous findings of maximal local gamma power elicited by object categorization paradigms—parietal for induced GBA (Gruber et al.,

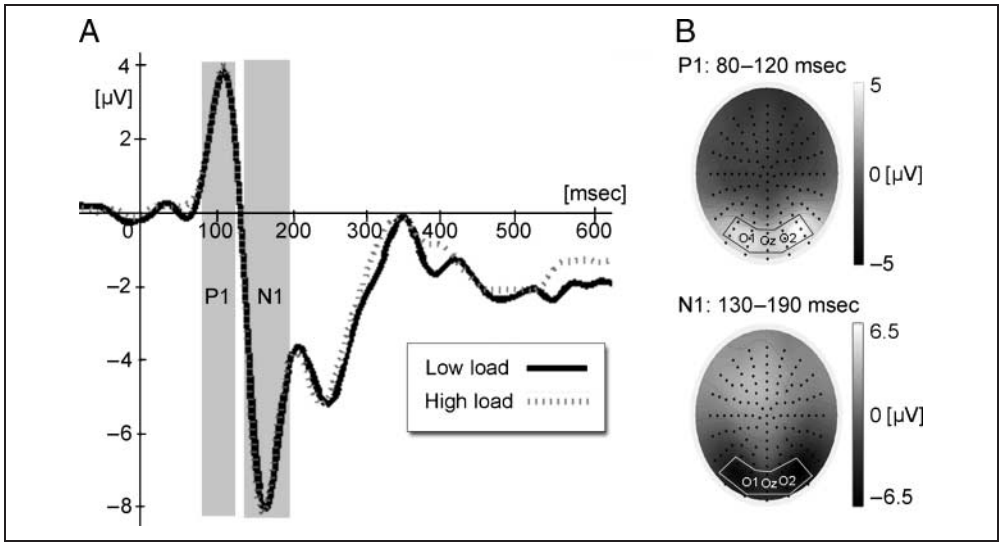

Figure 2. (A) Grand-mean baseline-corrected ERP waveforms averaged across electrodes. Shaded areas indicate components of interest. (B) Scalp topographies of P1 and N1 components reflecting grand-mean data averaged across all conditions. Boxes indicate electrode sites included in the regional mean. Note: different voltage scales.

2004) and occipital for evoked GBA (Tallon-Baudry, Bertrand, Delpuech, & Pernier, 1997). These sites were to be readjusted in order to envelop the area of maximal amplitude in case the observed grand-mean topography happened to differ from previous findings. To depict these topographies, wavelet analysis was recalculated for all 128 electrodes. Maps of oscillatory responses were calculated for both conditions by means of spherical spline interpolations (Perrin, Pernier, Bertrand, & Echallier, 1998). These maps represented an average of activity in the ±5 Hz frequency band centered upon the maximal power wavelet for each participant during the time window of maximal acitivity.

For both types of GBA, the time window of highest gamma amplitude was identified for the purposes of the analysis. The length of this time window was defined based on the observed grand-mean GBA, a common approach in previous studies (e.g., Gruber & Müller, 2005; Busch et al., 2004).

In order to identify the time window and frequency range of the induced GBA peaks, mean baseline-corrected spectral amplitude (baseline: 100 msec prior to stimulus onset) was collapsed for all conditions together and represented in TF plots in the 30–90 Hz range. Regional means of interest were then selected on the basis of grand-mean topographies. Due to interindividual differences in the induced gamma peak in the frequency domain, a specific wavelet for each participant was chosen, designed for the frequency of his or her maximal amplitude in the gamma range based upon an average across both low and high load conditions. Centered upon this wavelet, a frequency band of ±5 Hz was subsequently formed for statistical analysis.

By definition, evoked oscillatory activity is phase-locked to stimulus onset and was analyzed through a transformation of the unfiltered ERP into the frequency domain. Evoked GBA is a response with low interindividual variability in latency at frequencies between 30 and 40 Hz, with maximal activity usually occurring in a narrow time interval around 100 msec poststimulus onset. Therefore, a ±5 Hz range was taken around a central wavelet of 35 Hz within a time window of 50 to 150 msec.

In short, GBA was analyzed in the ±5 Hz frequency band around the wavelets of interest; 35 Hz for evoked GBA and individual maximal wavelet for induced GBA. Means and standard errors (*SE*s) of the mean are reported throughout the Results section. Differences against baseline in GBA amplitude at the site of the regional mean during the time window of maximal activity were tested using independent *t* tests against zero.

Results

Behavioral Data

Mean error rates and their *SE*s were as follows: low perceptual load = 3.1 ± 0.5% and high perceptual load = 12.3 ± 1.7%. Mean RTs and their *SE*s, computed only from correctly answered items, were as follows: low load = 652 ± 27 msec and high load = 848 ± 24 msec. Highly significant effects were found with more errors and longer response latencies for higher load [error rate: $t(12) = -5.76$, $p < .001$; RTs: $t(12) = -14.56$, $p < .001$].

Event-related Potentials

Figure 2 depicts the ERPs. There were no significant effects of perceptual load on either of the components. Both P1 and N1 were maximal at occipital sites. P1 had a grand-mean baseline-corrected amplitude of 1.95 ± 0.39 μV for low and 1.99 ± 0.31 μV for high perceptual load [$t(11) = -0.20$, *ns*]. N1 had a grand-mean baseline-corrected amplitude of −3.47 ± 0.75 μV for low and −3.46 ± 0.72 μV for high perceptual load [$t(11) = -0.03$, *ns*].

Evoked and Induced Spectral Changes

Figure 3 shows grand-mean baseline-corrected TF plots and topographies of event-related GBA collapsed across experimental conditions.

Gamma-band amplitude *evoked* by stimulus presentations between 30 and 40 Hz during a time window of 50 to 150 msec showed a slight increase at occipital sites (Figure 3A) throughout the lower gamma frequency ranges. This increase was not significant for either low load [0.05 ± 0.04 μV, $t(11) = 1.22$, *ns*] or high load [0.004 ± 0.03 μV, $t(11) = 0.16$, *ns*].

Spectral amplitude *induced* by stimulus presentations showed a slight enhancement in a time window from approximately 170 to 410 msec after stimulus onset in a frequency range between 30 and 80 Hz (Figure 3B). This enhancement was also not significant when tested against zero for either low load [0.01 ± 0.03 μV, $t(11) = 0.25$, *ns*] or high load [0.04 ± 0.03 μV, $t(11) = 1.32$, *ns*].

Conclusion

Behavioral effects of perceptual load were obtained both in error rates and RTs. Early ERP components P1 and N1 were not significantly modulated by perceptual load. This confirms our hypothesis and is in accordance with Handy et al.'s (2001) predictions that, under constant attentional allocation, the early effects of load should be eliminated. It was also determined that low and high load local form stimuli did not produce significant enhancements in either evoked or induced GBA. This leads to the conclusion that the matching tasks of either low or high load do not have the capacity to elicit significant event-related GBA, such as the one usually

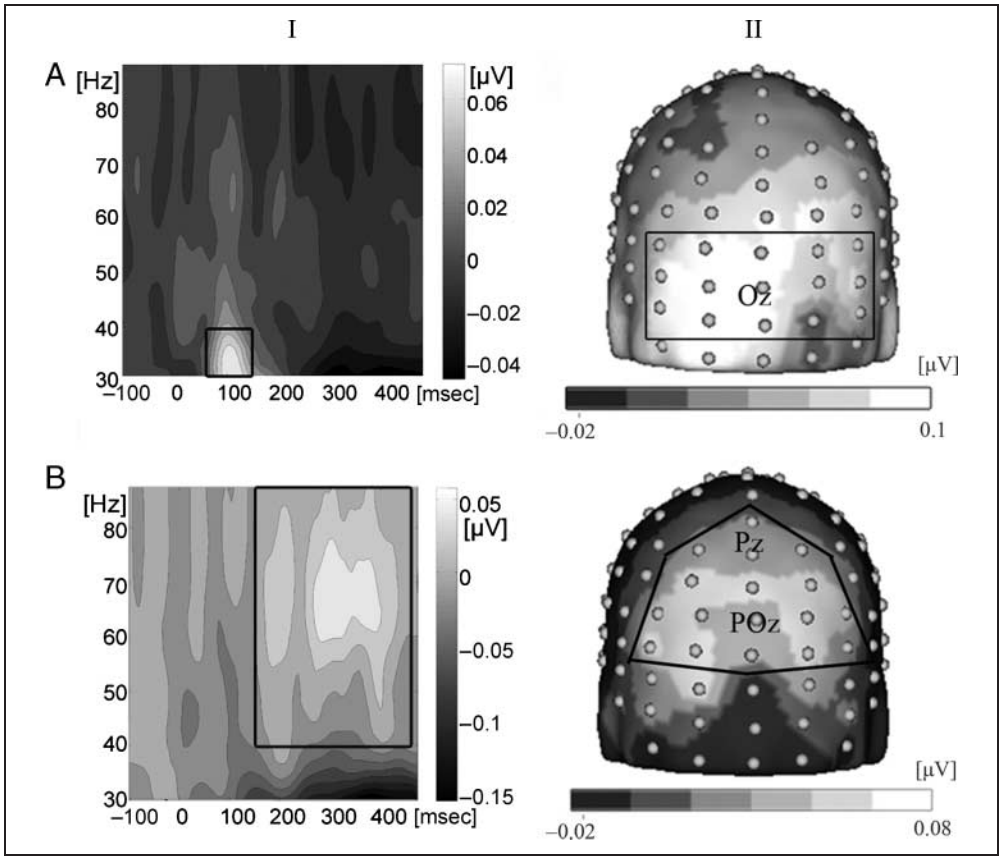

Figure 3. Evoked (A) and induced (B) GBA. (I) Grand-mean baseline-corrected TF plots averaged across 128 electrodes and all conditions. Black boxes indicate the time window for statistical analysis. (II) Grand-mean 3-D spherical spline amplitude maps (averages across all conditions) based on the ±5 Hz frequency band centered on the wavelet of interest (35 Hz for evoked, individual maximal wavelet for induced) during the selected time window. Black boxes indicate electrode sites included in the regional mean.

observed in object recognition tasks, when presented in isolation.

EXPERIMENT 2

In Experiment 2, the local form stimuli of low and high perceptual load were copresented with either familiar or unfamiliar task-irrelevant objects. Behavioral effects of load in the absence of effects of distractor type were expected as these have been observed in previous studies, where load varied from trial to trial (e.g., Murray & Jones, 2002). To repeat the crucial hypotheses, induced GBA elicited by presentations of familiar as opposed to unfamiliar objects was expected to show enhancements, driven by increases in activity under low load. Additionally, it was expected that evoked GBA would dissociate from induced GBA by showing enhancements with increases in perceptual load, irrespective of distractor type.

Methods

Participants

Nineteen participants took part. Three had to be removed from the sample due to excessive EEG artifacts. The remaining 16 (4 men), aged 19 to 46 years (mean age = 24.5 years) were all healthy, right-handed university students and received class credit or a small honorarium for participation. Participants reported normal or corrected-to-normal vision. Individual written informed consent was obtained and the study conformed to the Code of Ethics of the World Medical Association.

Materials and Procedure

The central stimuli from Experiment 1 were superimposed over a background that could contain either a familiar object or an unfamiliar object. The unfamiliar objects were created from familiar objects by image distortion (see Figure 4 for examples). Intersecting the factors of load and familiarity, four conditions were formed: low load familiar, low load unfamiliar, high load familiar, and high load unfamiliar. Ninety-six stimuli were shown for each of the four conditions. As the object set contained 384 images, each of the 192 local form stimuli were shown twice during the experiment and were assigned to two pairs of images, familiar and unfamiliar.

The objects in the images were 1.4° to 4.5° of visual angle in size. The presentation was randomized and counterbalanced to ensure that if one participant saw one half of the images in familiar and the other half in unfamiliar form, a second matched participant would see them presented in opposite conditions, that is, if one saw the ''cat'' the other would see the distorted version of the ''cat.''

The experiment consisted of four blocks lasting approximately 5 min and containing 96 trials each. Each

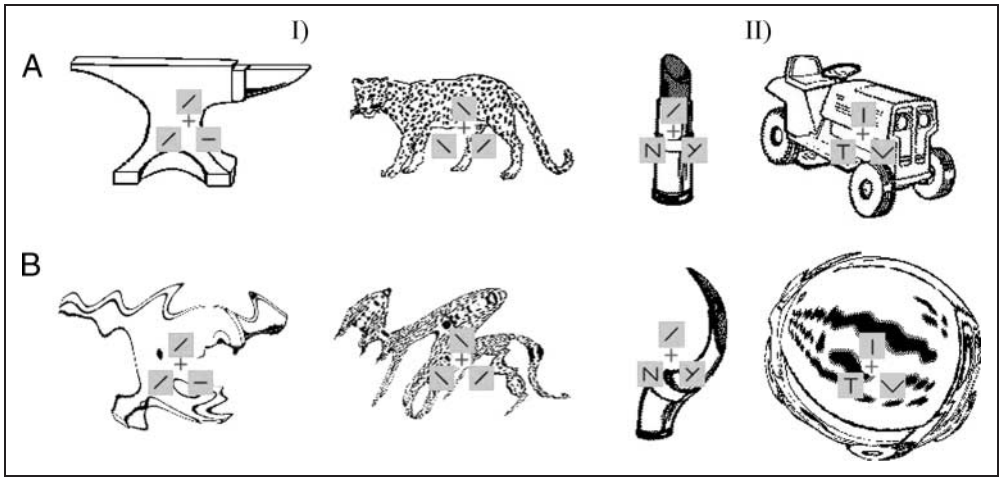

Figure 4. Examples of stimuli. (A-I) Low load, familiar objects; (A-II) high load, familiar objects; (B-I) low load, unfamiliar objects; (B-II) high load, unfamiliar objects.

trial consisted of a variable 500–800 msec baseline period during which a red fixation cross (0.2° × 0.2°) was presented. This was followed by a stimulus picture that was displayed for 650 msec. The picture was then replaced by the fixation cross which remained on the screen for a period of 750 msec (see Figure 5 for trial outlook).

The experiment used the same tools and equipment as Experiment 1. Stimulus presentation setup and response collection were also the same. Participants were instructed to perform the task as in Experiment 1 and were told to ignore the irrelevant background images.

EEG Recording

The average rejection rate in this experiment was 25.9% resulting in an average of approximately 64 remaining trials per condition (For general information on EEG recording procedure, see Methods section for Experiment 1).

Behavioral Data Analysis

RTs between 250 and 1400 msec (the maximum time allowed for responses) after stimulus onset on trials with correct responses were taken into further analysis. Mean RTs and error rates were computed for each participant. Differences in error rates and response speed between conditions were analyzed with a 2 × 2 repeated measures analysis of variance (ANOVA) with the within-subject factors of perceptual load (low and high) and distractor type (familiar or unfamiliar object).

Event-related Potentials Analysis

As in Experiment 1, a 25-Hz low-pass filter was applied to the data before all ERP analyses. Two early (P1, N1) and two late (L1, L2) ERP components were assessed. For each component, regional means (shown in Figure 6; see Results) were assigned to areas encompassing maximal activity electrodes when data were collapsed across conditions. Average amplitudes across electrodes at these sites in the respective time window (see Table 1 and Results section) were then computed and the mean amplitude during the period 100 msec prior to stimulus onset (baseline) was subtracted. Mean latencies were not analyzed because no differences were predicted. Each component was subject to a 2 × 2 repeated measures ANOVA comprising the within-subjects factors of perceptual load (low and high) and distractor type (familiar and unfamiliar objects). Means and standard error rates are reported throughout the Results section. Post hoc tests were performed using paired *t* tests.

Analysis of Evoked and Induced Spectral Changes

Oscillatory activity was analyzed according to the same general procedure described in the Methods section of Experiment 1. The time windows and regional means were selected on the basis of grand-mean TF plots and topographies, and GBA was analyzed in the ±5 Hz frequency band around the wavelets of interest; 35 Hz for evoked GBA and individual maximal wavelet for induced GBA. The evoked GBA did not exhibit a specific peak and, therefore, a 30- to 40-Hz range was chosen in order to make the findings comparable to previous studies (Gruber & Müller, 2005; Herrmann, Lenz, et al., 2004).

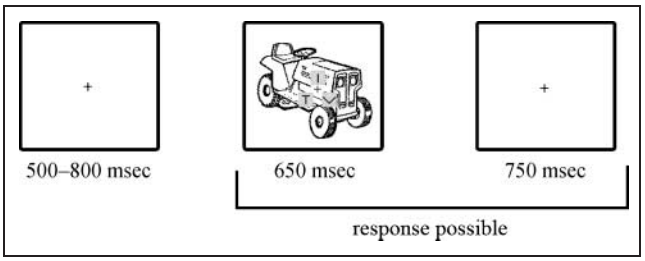

Figure 5. Trial outlook for Experiment 2.

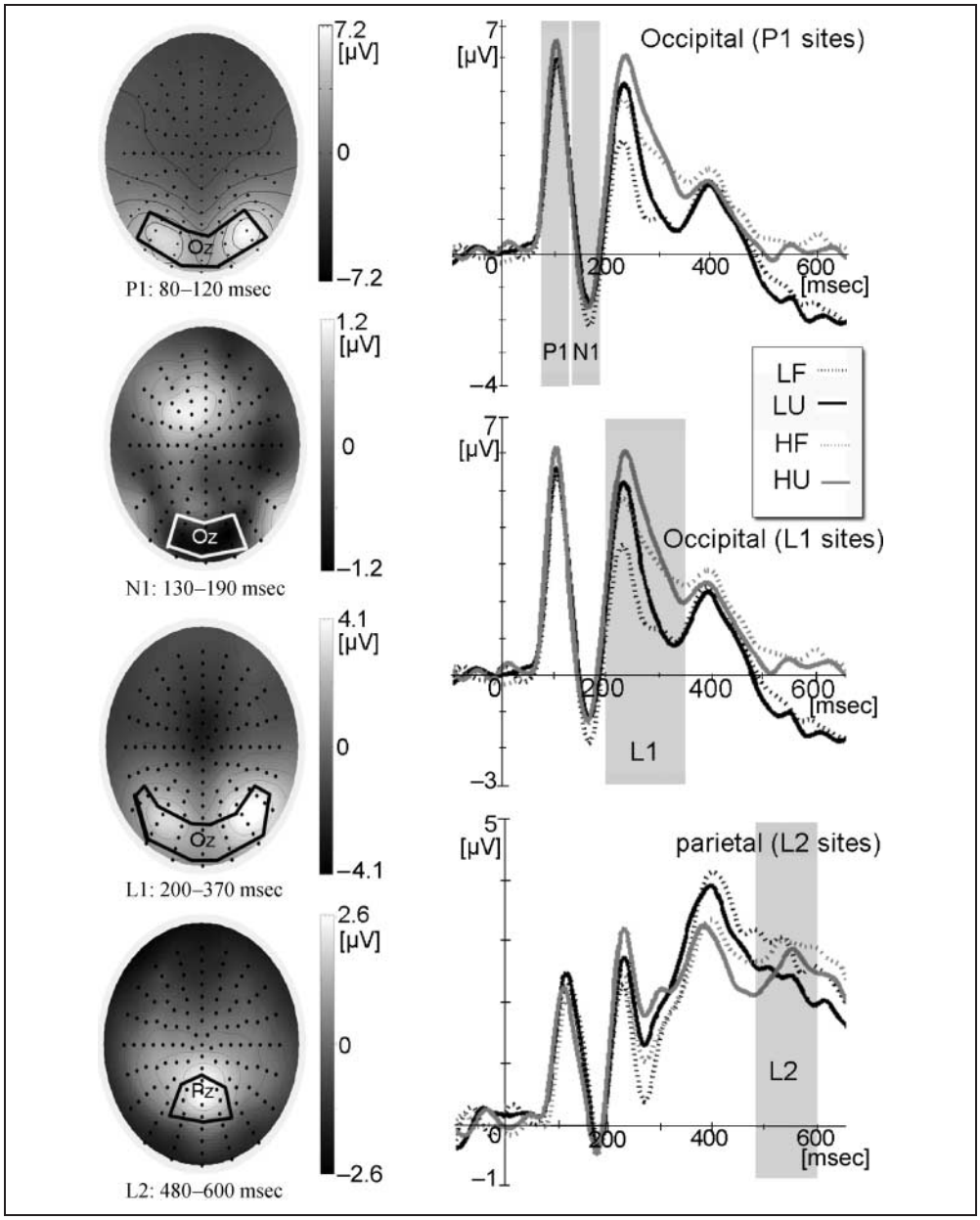

Figure 6. Left: Scalp topographies of P1, N1, L1, and L2 from grand-mean data averaged across all conditions. Boxes indicate electrode sites included in regional means. Right: Grand-mean baseline-corrected ERP waveforms at the regional means. Shaded areas indicate components of interest. (LF = low load familiar; LU = low load unfamiliar; HF = high load familiar; HU = high load unfamiliar). Note: different voltage scales; also note that P1 and N1 both are shown at P1 sites only as there is considerable overlap resulting in highly similar waveforms.

In order to obtain differential activity in the gamma band that reflected object-specific processing, activity elicited by unfamiliar objects was subtracted from the activity elicited by familiar objects within every load level (i.e., low load familiar minus low load unfamiliar; high load familiar minus high load unfamiliar). The same procedure was employed to obtain differential activity in the gamma band related to task demands only, with

Table 1. ERP Components: Time Windows and Mean Baseline-corrected Amplitudes (n = 16)

		Low Perceptual Load Amplitude [μV] (Mean ± SE)		*High Perceptual Load Amplitude [μV] (Mean ± SE)*	
Component	*Time Window (msec)*	*Unfamiliar*	*Familiar*	*Unfamiliar*	*Familiar*
P1	80–120	3.08 ± 0.61	2.93 ± 0.54	3.33 ± 0.65	2.88 ± 0.64
N1	130–190	−0.18 ± 0.86	−0.42 ± 0.93	−0.43 ± 0.94	−0.29 ± 0.89
L1	200–370	2.01 ± 0.94	1.45 ± 0.91	2.85 ± 0.93	2.52 ± 0.89
L2	480–600	−0.15 ± 0.68	0.26 ± 0.60	0.65 ± 0.53	0.98 ± 0.57

activity elicited by low load subtracted from activity elicited by high load tasks within every object familiarity level (i.e., high load unfamiliar minus low load unfamiliar; high load familiar minus low load familiar). The sites with maximal amplitude changes between conditions were identified from the topographies of differential activity obtained by the subtractions. GBA amplitude was tested at these sites with a 2 × 2 repeated measures ANOVA with the within-subject factors of perceptual load (low and high) and distractor type (familiar or unfamiliar object). Tests were performed on the activity in the ±5 Hz frequency band around each participant's maximal wavelet for induced GBA and on the activity in the 30- to 40-Hz range for evoked GBA. Subtractions of GBA elicited by different conditions have already been used in studies that employed stimuli which were highly comparable between conditions (e.g., the colored checkerboards used in the attentional study by Müller & Keil, 2004). Such subtractions make it possible to isolate the activity related to a specific function. It was expected that the overall amplitudes in Experiment 2 would be rather small, as the small visual material for the matching task (Experiment 1) and unfamiliar objects (Gruber & Müller, 2005) elicits very little event-related GBA on their own. By topographically localizing the differences between closely matched conditions, load or familiarity, one is able to maximize the signal by focusing on the aspects that are most likely to reflect the representational processes of interest. Means and standard errors are reported throughout.

Results

Behavioral Data

Mean error rates with *SE*s were as follows: low load unfamiliar object, 2.2 ± 0.5%; low load familiar object, 1.9 ± 0.3%; high load unfamiliar object, 11.8 ± 1.4%; and high load familiar object, 13.6 ± 1.7%. Mean RTs with *SE*s were: low load unfamiliar object, 699 ± 14 msec; low load familiar object, 705 ± 15 msec; high load unfamiliar object, 916 ± 14 msec; and high load familiar object, 925 ± 17 msec. There were no interactions between the two factors of perceptual load and distractor type [error rates: $F(1, 15) = 1.56$, *ns*; RTs: $F(1, 15) = 0.13$, *ns*]. There was a main effect of perceptual load with a very significant increase in errors [$F(1, 15) = 82.6$, $p < .001$] and slowing of responses for high as opposed to low load [$F(1, 15) = 912.38$, $p < .001$]. The factor of distractor type had no effect on error rates [$F(1, 15) = 0.86$, *ns*] or speed of responding [$F(1, 15) = 2.7$, $p = .12$].

Event-related Potentials

Figure 6 depicts the ERP components and Table 1 provides information on their properties. A 2 × 2 repeated measures ANOVA was used to compare across conditions (perceptual load; distractor type).

P1 was maximal at occipital sites and showed no interaction between the two factors [$F(1, 15) = 1.58$, *ns*] and no main effect of load [$F(1, 15) = 0.78$, *ns*]. There was an effect of distractor type [$F(1, 15) = 5.34$, $p < .05$] being enhanced under high load for unfamiliar items in comparison to familiar items [$t(15) = 2.27$; $p < .05$]. There were no modulations of the N1 component [load: $F(1, 15) = 0.21$, *ns*; distractor type: $F(1, 15) = 0.08$, *ns*; interaction of the two factors: $F(1, 15) = 1.41$, *ns*]. L1 was modulated both by load [$F(1, 15) = 31.45$, $p < .001$], being enhanced for unfamiliar items, and by distractor type [$F(1, 15) = 8.19$, $p < .05$], being enhanced for high load stimuli. There was no interaction between the two factors [$F(1, 15) = 1.50$, *ns*]. L2 was enhanced under high load [$F(1, 15) = 8.52$, $p < .05$] with a modulation by distractor type [$F(1, 15) = 4.06$, $p = .06$] that approached statistical significance. There was a trend for enhancements for familiar objects under low load [$t(15) = -1.97$, $p = .07$].

Evoked and Induced Spectral Changes

Figure 7A shows grand-mean baseline-corrected TF plots for *evoked* GBA. Figure 7B shows the topography for data collapsed across experimental conditions. Figure 7C shows grand-mean amplitudes at the regional mean for each condition. Figure 7D shows topographies of the grand means of subtractions between levels of evoked GBA denoting object specificity within every load type, familiar minus unfamiliar, or task specificity within every distractor type, high load versus low load. Figure 7E shows grand-mean amplitudes for each condition at the sites of maximal differences represented in Figure 7D.

Gamma-band amplitude evoked by picture presentations during a time window of 50–150 msec showed an increase at occipital sites in the 30- to 40-Hz gamma-frequency range (Figure 7A and C). This activity extended into the lower frequencies, up to 20 Hz, in accordance with findings on evoked GBA in visual information processing tasks (Keil, Stolarova, Heim, Gruber, & Müller, 2003). When tested against zero, as shown in Figure 7B, above-baseline activity was found for low load familiar [$t(15) = 2.43$, $p < .05$] and for both high load conditions [unfamiliar: $t(15) = 3.14$, $p < .01$; familiar: $t(15) = 2.83$, $p < .05$]. Significant evoked GBA increases against baseline were not observed for low load unfamiliar objects [$t(15) = 1.5$, *ns*].

Subtractions within load type and distractor type revealed that maximal differences in activity were situated at central occipital sites (Figure 7D). A 2 × 2 repeated measures ANOVA showed that activity at these sites in the 30–40 Hz range (Figure 7E) remained unmodulated by object familiarity [$F(1, 15) = 0.05$, *ns*] or perceptual load [$F(1, 15) = 1.57$, *ns*].

Figure 8A shows grand-mean baseline-corrected TF plots for *induced* GBA. Figure 8C shows the topography for grand-mean data collapsed across experimental

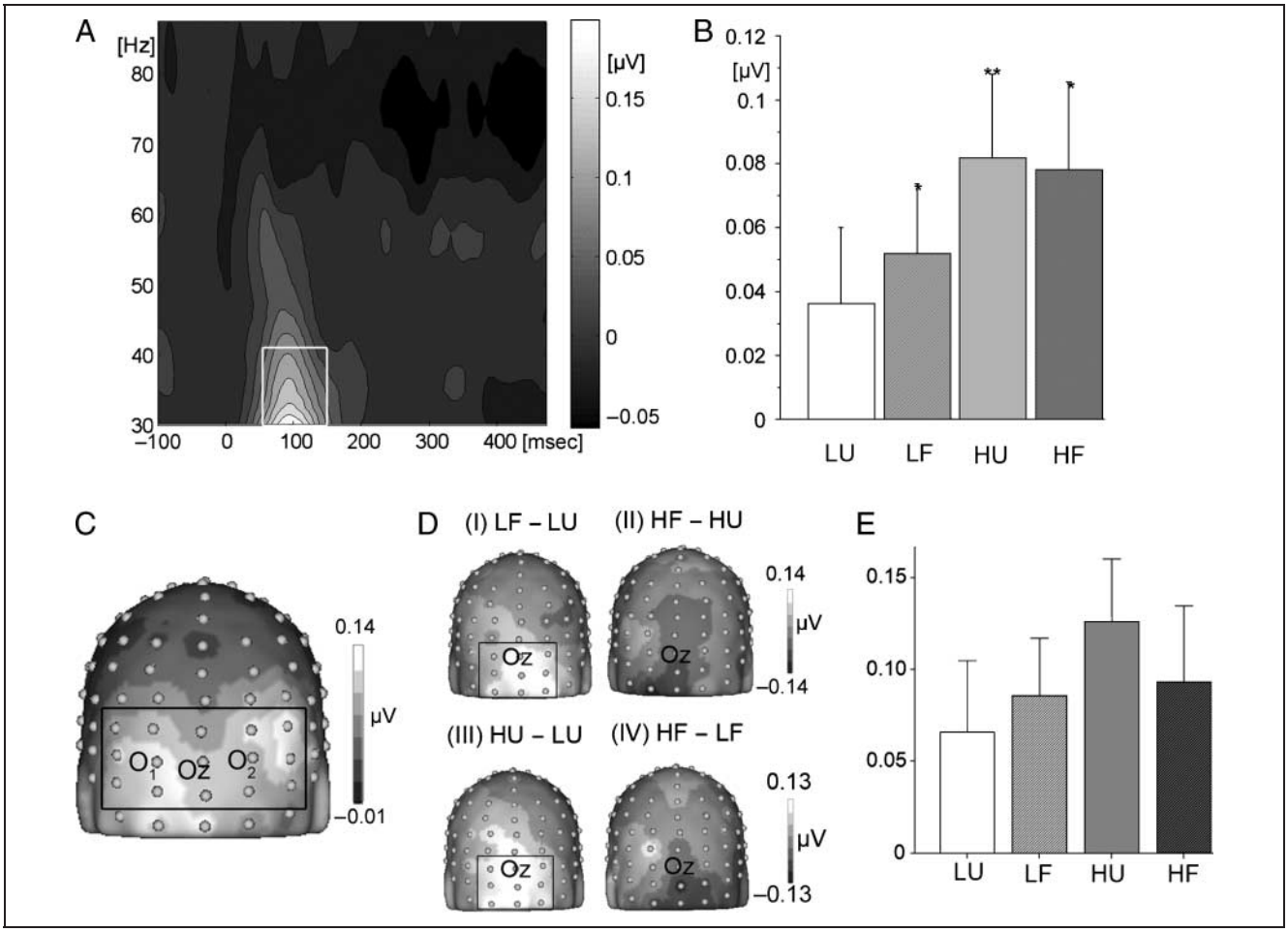

Figure 7. Evoked GBA. (A) Grand-mean baseline-corrected TF plot averaged at the regional mean sites (see B) across all conditions. Box indicates the time window for statistical analysis. (B) Bar plot of amplitudes of evoked GBA for each condition at the regional mean during the selected time window, with *SE* bars. (C) Grand-mean 3-D spherical spline amplitude map (average across all conditions) based on the ±5 Hz frequency band centered on the 35-Hz wavelet during the selected time window. Box indicates electrode sites included in the regional mean. (D) Grand-mean 3-D spherical spline amplitude maps of subtractions performed to isolate object-specific activity for each load (I and II) and load-specific activity for each distractor type (III and IV). Amplitude maps are based on subtractions of grand-mean baseline-corrected amplitudes within the ±5 Hz frequency bands centered on the 35-Hz wavelet during the selected time window; sites of maximal differences are indicated by the box (LF = low load familiar; LU = low load unfamiliar; HF = high load familiar; HU = high load unfamiliar). (E) Bar plot of amplitudes of evoked GBA for each condition at the sites of maximal differences during the selected time window, with *SE* bars. * indicates significance against zero at $p < .05$, ** at $p < .01$. Note: different voltage scales.

conditions. Figure 8B shows grand-mean amplitudes at the regional mean (defined as electrode sites with maximal activity; see Figure 8C) for each condition separately. Figure 8D shows topographies of grand-mean subtractions between levels of induced GBA denoting object specificity within every load type, familiar minus unfamiliar, or task specificity within every distractor type, high load minus low load. Figure 8E shows grand-mean amplitudes for each condition at the sites of maximal differences represented in Figure 8D.

Spectral amplitude induced by picture presentations showed an enhancement in a time window from approximately 170 to 450 msec after stimulus onset in a frequency range between 40 and 90 Hz (Figure 8A). This enhancement was highly significant when tested against zero for the low load familiar object condition [$t(15) = 4.83$, $p < .001$], although it was not significant for the low load unfamiliar object condition [$t(15) = 1.44$, *ns*]. Both high load conditions elicited induced GBA which was significantly increased compared to baseline [unfamiliar object: $t(15) = 2.72$, $p < .05$; familiar object: $t(15) = 3.38$, $p < .005$].

Differential task-specific activity was computed by subtracting induced GBA elicited by low load tasks from the induced GBA elicited by high load tasks for each participant and then calculating a grand mean across participants to obtain task-related activity within every distractor type. The same type of subtractions (familiar minus unfamiliar object) was performed within every perceptual load level to obtain object-specific activity in the induced GBA. Figure 8D shows that the highest differences were centered on left parieto-occipital sites.

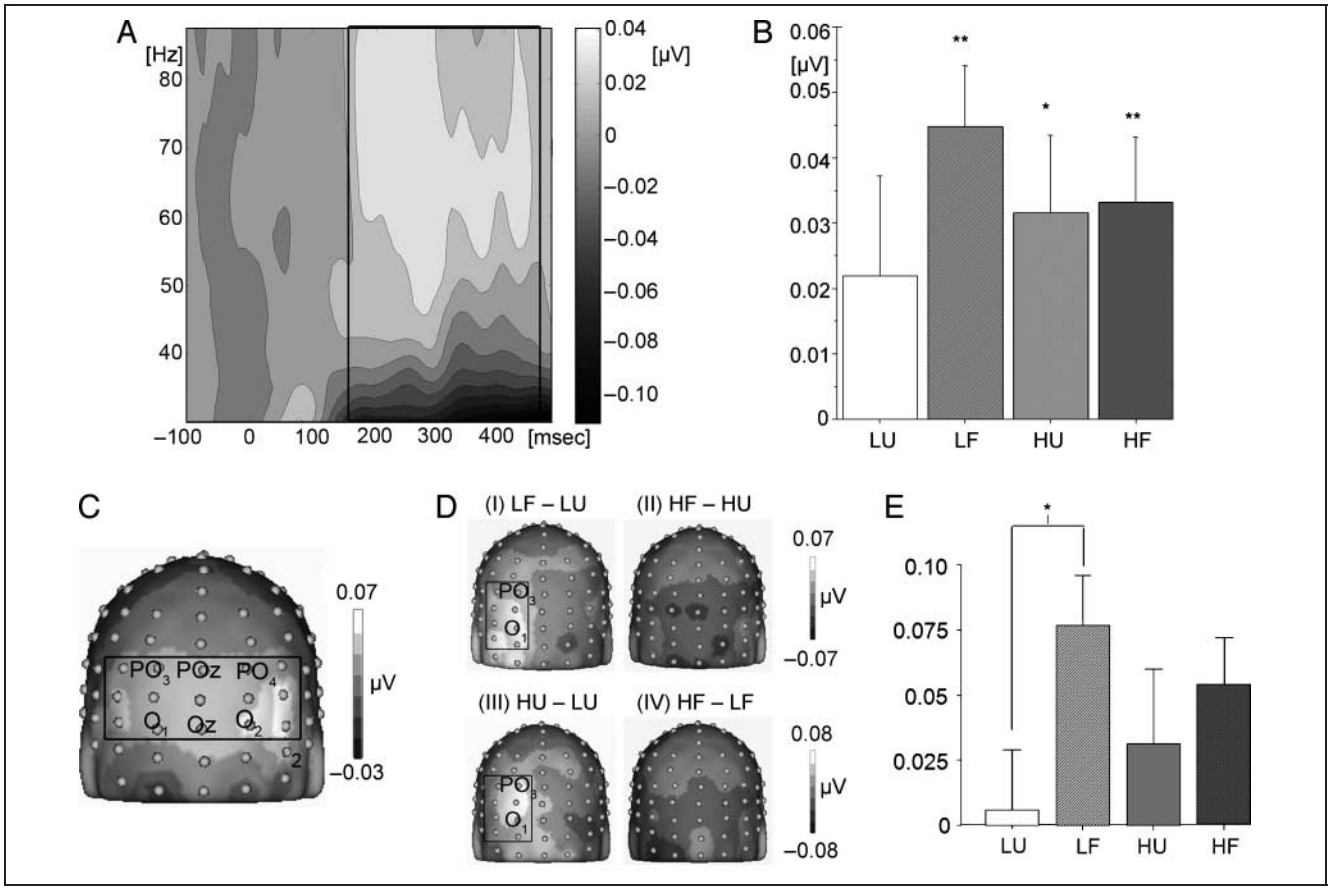

Figure 8. Induced GBA. (A) Grand-mean baseline-corrected TF plot averaged at the regional mean (see B) across all conditions. Box indicates the time window for statistical analysis. (B) Bar plot of amplitudes of induced GBA for each condition at the regional mean during the selected time window, with *SE* bars. (C) Grand-mean 3-D spherical spline amplitude map (average across all conditions) based on the ±5 Hz frequency band centered on the maximal individual wavelet for each participant during the selected time window. Box indicates electrode sites included in the regional means. (D) Grand-mean 3-D spherical spline amplitude maps of subtractions performed to isolate object-specific activity for each load (I and II) and load-specific activity for each distractor type (III and IV). Amplitude maps are based on subtractions of grand-mean baseline-corrected amplitudes within the ±5 Hz frequency bands centered on the wavelet of interest during the selected time window; sites of maximal differences are indicated by the box (LF = low load familiar; LU = low load unfamiliar; HF = high load familiar; HU = high load unfamiliar). (E) Bar plot of amplitudes of evoked GBA for each condition at the sites of maximal differences during the selected time window, with *SE* bars. * indicates significance against zero at $p < .05$, ** at $p < .01$. Note: different voltage scales.

When the activity at these sites (Figure 8E) was tested with a 2 × 2 repeated measures ANOVA, a highly significant main effect of object familiarity was found [$F(1, 15) = 8.75$, $p < .01$]. This effect was mostly driven by increases in induced GBA under low load [$t(15) = -2.25$, $p < .05$], whereas the object-specific change under high load was not significant [$t(15) = -0.56$, *ns*]. There was no main effect of task demands [$F(1, 15) = 0.02$, *ns*].

From comparisons between Figures 7B and 8B and the *t* tests against zero, it is clear that induced GBA was most significantly enhanced for familiar objects under low load. Evoked GBA amplitude was most significantly enhanced for high load items. Although induced GBA amplitude was significantly enhanced by object familiarity at left parieto-occipital sites (Figure 8E), occipital evoked GBA remained unmodulated (Figure 7E). Post hoc tests have shown that object-specific increases in induced GBA were most evident under low perceptual load.

DISCUSSION

In line with previous studies (Lavie et al., 2004; Murray & Jones, 2002; Lavie, 1995), the obtained behavioral results exhibited main effects of load but not of distractor type, suggesting that the attentional focus was consistently assigned to the central stimuli in both low and high load conditions. In line with these findings, the early components P1 and N1 were not modulated by load, thus confirming Handy et al.'s (2001) predictions. Therefore, we conclude that, throughout the experiment, attention was equally allocated to the central stimuli irrespective of perceptual load.

The role of event-related GBA as a neural marker of representational processing of unattended objects can

therefore be appraised. According to our hypotheses, some representational processing of unattended objects should occur under conditions of low perceptual load and induced GBA should be a marker of this object-specific activity. In fact, none of the studied ERP components (P1, N1, L1, and L2) showed any specific modulations by object familiarity under low load. Significant levels of evoked GBA always preceded enhancements in induced GBA, as predicted by Herrmann, Munk, et al. (2004). However, evoked GBA failed to show any significant modulations. The only component that showed specific sensitivity to object familiarity was the induced GBA. This object-specific activity was centered at left parieto-occipital sites; this was especially pronounced when perceptual load was low.

A series of studies had previously failed to find any differential processing of familiar against unfamiliar objects in the evoked GBA (Gruber et al., 2006; Fiebach et al., 2005; Gruber & Müller, 2005; Tallon-Baudry et al., 1996). On the contrary, Herrmann, Munk, et al. (2004) and Fründ et al. (2008) observed significant increases in evoked GBA for familiar objects as opposed to unfamiliar objects. Discrepancies may arise due to different modes of object processing that depend on both the task and the stimulus material. Incidental processing of objects can be bottom–up driven, relying on image features that are unique to salient object configurations; for example, the geometrical stability and the qualities of elongation and symmetry axes specific to objects (see Marr, 1982). Evoked GBA is an early marker sensitive to both bottom–up and top–down influences (Busch, Schadow, et al., 2006) and is extremely responsive to object properties; even more so than early ERPs (Busch et al., 2004). On the basis of many studies on shape familiarity and figure–ground factors (Peterson & Gibson, 1993, 1994a, 1994b; for an overview, see Peterson & Skow-Grant, 2003), it was concluded that object memories constitute a configural cue that contributes to early perceptual organization. Further research should focus on the importance of task relevance of object identity because this is likely to play a crucial role in determining whether evoked GBA shows a more bottom–up effect of configural processing (Herrmann, Munk, et al., 2004) or a more top–down effect of task relevant processing of image's features for the purpose of identification (Gruber et al., 2006; Fiebach et al., 2005; Gruber & Müller, 2005; Tallon-Baudry et al., 1996).

This study did not support the hypothesis that evoked GBA would be a sensitive marker for increases in task demands. This negative finding is similar to Posada et al.'s (2003) study, which found no effects of task complexity on evoked GBA by contrasting a simple color-to-button visual association task with a more complex rule-based task. It runs contrary to Senkowski and Herrmann's (2002) finding that increased task complexity augments evoked GBA. Senkowski and Herrmann contrasted a complex task to a passive viewing task, which suggests that changes in demand need to be sufficiently large in order to modulate evoked GBA amplitude. Posada et al. found an effect of task complexity on induced gamma-band oscillations at right parietal sites and explained it by additional attentional top–down influences introduced by the need to perform a rule operation in the complex task. In the current study, due to randomly intermixed trials of low and high load, attention remained constrained to the local form stimuli by top–down influences. This explains why induced GBA remained unmodulated by changes in task demands between the low and high load.

It is also necessary to contrast Experiment 1, which found no significant GBA for low or high load tasks in isolation, with Experiment 2, which found that both evoked and induced GBA were significantly enhanced against baseline when high load distractors were paired with unfamiliar objects. This implies that a simple increase in the complexity of the stimulus results in above-baseline increases in activity. These enhancements are likely to be an outcome of more intense suppression of the surrounding spatially coexistent distractors while performing a perceptually demanding high load task. This explanation is in accordance with the biased competition model of attention, which applies in particular to the processing within the ventral visual stream responsible for object recognition (e.g., see Desimone, 1998). It suggests that the competition arising from more complex stimulus configurations could, in itself, result in enhanced levels of event-related GBA. This is not surprising because synchronization of responses in the visual cortex at the frequencies of 20–65 Hz has been shown to result from intercortical coupling mechanisms whose effectivity rises as central activation increases (Herculano-Houzel, Munk, et al., 1999). Furthermore, neurons which receive the inhibitory postsynaptic potentials of GABAergic interneurons form the root of these high-frequency components in network-driven synaptic activity because their potentials carry more synchronicity and power in the gamma-band range (Hasenstaub, Shu et al. 2005). Interneuronal involvement has also been explicitly acknowledged by the representational hypothesis of Tallon-Baudry and Bertrand (1999). Similarly, a modulation of the P1 by distractor type was also found in this study, with specific enhancements for unfamiliar objects under high load. This leads to the supposition that an interplay between concurrent early enhancement of central task-relevant information and suppression of colocalized distractors might reflect on the P1 effect (Luck, 1995).

Returning to the crucial finding that induced GBA is the only object-specific marker of representational neural processing, ERP components L1 and L2, that relate to the processing of objects, did not show such specificity. The late ERP component L1 was modulated by object familiarity and load, being monotonously enhanced both for high load and for unfamiliar objects. L1 enhancements

for unfamiliar objects are in line with previous findings (Gruber & Müller, 2005). The late component L2 showed a trend to increase under high load for familiar objects. This supports Gruber and Müller (2005), who also found a trend toward L2 enhancements for repetitions of familiar objects showing that this late component, related to semantic processing, is responsive to familiar object identities. These robust ERP findings are in accordance with existing literature but this study's main contribution lies in its ability to demonstrate that induced GBA is the most relevant marker of representational processing of unattended objects. This further strengthens Tallon-Baudry and Bertrand's (1999) representational hypothesis, which claims that induced GBA is a neural marker of cortical object representation.

Increases in induced GBA for familiar objects were driven by enhancements in activity under low load in accordance with Lavie's (1995) model. This model claims that high load effectively reduces distractor perception and predicts that under high load no priming should be possible. Because induced GBA is a priming-sensitive component (Fiebach et al., 2005; Gruber & Müller, 2002, 2005; Gruber et al., 2004), the lack of object-specific effects under high load could also have been predicted, thus further supporting the representational hypothesis.

Finally, the lack of object-specific effects under high load has important implications for the role of attentional selection in visual representation of objects. High load conditions with foveally colocalized items can be perceived as a simplified model of object processing in complex visual scenes. From our findings, it is clear that selective attention does have a crucial role to play in the processing of objects under high perceptual demands. Such high demands loosely approximate everyday situations, in which the visual system is faced with multitudes of ambiguous, cluttered visual scenes. Objects under low load conditions seem to hold a privileged status in the processing hierarchy and can capture perceptual resources, which is reflected in specific increases of induced GBA. Under high load conditions, however, processing is determined by perceptual mechanisms of attentional selection. In situations that involve competition between different stimuli, these mechanisms ensure the most efficient processing of attended content with a general suppression of surrounding information. Taken together, this evidence further supports the idea that high-frequency oscillatory synchrony, and in particular its induced component, is likely to be a fundamental mechanism both for automatic coherent percept formation and for perceptual information processing and attentional selection, also evidenced in a recent magnetoencephalographic study on induced GBA (Vidal, Chaumon, O'Regan, & Tallon-Baudry, 2006). As object coding is heavily reliant on perceptual, mnemonic, and attentional processes, this explains why visual representation of objects is specifically marked by enhancements in induced high-frequency oscillatory synchrony.

Acknowledgments

We thank Renate Zahn and Tobias Forderer for help with data acquisition, Sophie Trauer for help with stimulus design and data acquisition, Søren Andersen for technical assistance, and Anthony Martyr for proofreading the manuscript. J. M. was supported by the Deutscher Akademischer Austausch Dienst (DAAD). The Deutsche Forschungsgemeinschaft also supported this research.

Reprint requests should be sent to Matthias M. Müller, Institut für Psychologie I, Universität Leipzig, Seeburgstrasse 14–20, 04103 Leipzig, Germany, or via e-mail: m.mueller@rz.uni-leipzig.de.

REFERENCES

Altmann, C. F., Grodd, W., Kourtzi, Z., Bülthoff, H. H., & Karnath, H.-O. (2005). Similar cortical correlates underlie visual object identification and orientation judgment. *Neuropsychologia, 43,* 2101–2108.

Beck, D. M., & Lavie, N. (2005). Look here but ignore what you see: Effects of distractors at fixation. *Journal of Experimental Psychology: Human Perception and Performance, 31,* 592–607.

Bertrand, O., & Pantev, C. (1994). Stimulus frequency dependence of the transient oscillatory auditory evoked response (40 Hz) studied by electric and magnetic recordings in human. In C. Pantev, T. Elbert, & B. Lütkenhöner (Eds.), *Oscillatory event-related brain dynamics* (pp. 231–242). New York: Plenum.

Busch, N. A., Debener, S., Kranczioch, C., Engel, A. K., & Herrmann, C. S. (2004). Size matters: Effects of stimulus size, duration and eccentricity on the visual gamma-band response. *Clinical Neurophysiology, 115,* 1810–1820.

Busch, N. A., Herrmann, C. S., Müller, M. M., Lenz, D., & Gruber, T. (2006). A cross-lab study of event-related gamma activity in a standard object-recognition paradigm. *Neuroimage, 33,* 1169–1177.

Busch, N. A., Schadow, J., Fruend, I., & Herrmann, C. S. (2006). Time-frequency analysis of target detection reveals an early interface between bottom–up and top–down processes in the gamma-band. *Neuroimage, 29,* 1106–1116.

Delorme, A., & Makeig, S. (2004). EEGLAB: An open source toolbox for analysis of single-trial EEG dynamics including independent component analysis. *Journal of Neuroscience Methods, 134,* 9–21.

Desimone, R. (1998). Visual attention mediated by biased competition in extrastriate visual cortex. *Philosophical Transactions of the Royal Society London, Series B, 353,* 1245–1255.

Duncan, J. (1980). The locus of interference in the perception of simultaneous stimuli. *Psychological Review, 87,* 272–300.

Fiebach, C. J., Gruber, T., & Supp, G. G. (2005). Neuronal mechanisms of repetition priming in occipitotemporal cortex: Spatiotemporal evidence from functional magnetic resonance imaging and electroencephalography. *Journal of Neuroscience, 25,* 3414–3422.

Fründ, I., Busch, N. A., Schadow, J., Gruber, T., Körner, U., & Herrmann, C. S. (2008). Time pressure modulates electrophysiological correlates of early visual processing. *PLOS Biology, 3,* e1675.

Gruber, T., Malinowski, P., & Müller, M. M. (2004). Modulation of oscillatory brain activity & evoked potentials in a repetition priming task in the human EEG. *European Journal of Neuroscience, 19,* 1073–1082.

Gruber, T., & Müller, M. M. (2002). Effects of picture repetition on induced gamma band responses, evoked potentials, and phase synchrony in the human EEG. *Cognitive Brain Research, 13,* 377–392.
Gruber, T., & Müller, M. M. (2005). Oscillatory brain activity dissociates between associative stimulus content in a repetition priming task in the human EEG. *Cerebral Cortex, 15,* 109–116.
Gruber, T., Müller, M. M., Keil, A., & Elbert, T. (1999). Selective visual–spatial attention alters induced gamma band responses in the human EEG. *Clinical Neurophysiology, 110,* 2074–2085.
Gruber, T., Trujillo-Barreto, J. N., Giabbiconi, C. M., Valdes-Sosa, P. A., & Müller, M. M. (2006). Brain electrical tomography (BET) analysis of induced gamma band responses during a simple object recognition task. *Neuroimage, 29,* 888–900.
Handy, T. C., & Mangun, G. R. (2000). Attention and spatial selection: Electrophysiological evidence for modulation by perceptual load. *Perception & Psychophysics, 62,* 175–186.
Handy, T. C., Soltani, M., & Mangun, G. R. (2001). Perceptual load and visuocortical processing: Event-related potentials reveal sensory-level selection. *Psychological Science, 12,* 213–218.
Hasenstaub, A., Shu, Y., Haider, B., Kraushaar, U., Duque, A., & McCormick, D. A. (2005). Inhibitory postsynaptic potentials carry synchronised frequency information in active cortical networks. *Neuron, 47,* 423–435.
Herculano-Houzel, S., Munk, M., Neuenschwander, S., & Singer, W. (1999). Precisely synchronized oscillatory firing patterns require electroencephalographic activation. *Journal of Neuroscience, 19,* 3992–4010.
Herrmann, C. S., Lenz, D., Junge, S., Busch, N. A., & Maess, B. (2004). Memory-matches evoke human gamma-responses. *BMC Neuroscience, 5,* 13.
Herrmann, C. S., Munk, M. H. J., & Engel, A. K. (2004). Cognitive functions of gamma-band activity: Memory match and utilization. *Trends in Cognitive Sciences, 8,* 347–355.
Hummel, J. E., & Stankiewicz, B. J. (1996). An architecture for rapid, hierarchical structural description. In T. Inui & J. McClelland (Eds.), *Attention and performance: XVI. Information integration in perception and communication* (pp. 93–121). Cambridge, MA: MIT Press.
Junghoefer, M., Elbert, T., Tucker, D. M., & Braun, C. (2000). Statistical control of artifacts in dense array EEG/MEG studies. *Psychophysiology, 37,* 523–532.
Karakas, S., & Basar, E. (1998). Early gamma response is sensory in origin: A conclusion based on cross-comparison of results from multiple experimental paradigms. *International Journal of Psychophysiology, 31,* 13–31.
Keil, A., Stolarova, M., Heim, S., Gruber, T., & Müller, M. M. (2003). Temporal stability of high-frequency brain oscillations in the human EEG. *Brain Topography, 16,* 101–110.
Lachter, J., Forster, K. I., & Ruthruff, E. (2004). Forty-five years after Broadbent (1958): Still no identification without attention. *Psychological Review, 111,* 880–913.
Lavie, N. (1995). Perceptual load as a necessary condition for selective attention. *Journal of Experimental Psychology: Human Perception and Performance, 21,* 451–468.
Lavie, N., Hirst, A., de Fockert, J. W., & Viding, E. (2004). Load theory of selective attention and cognitive control. *Journal of Experimental Psychology: General, 133,* 339–354.
Luck, S. J. (1995). Multiple mechanisms of visual–spatial attention: Recent evidence from human electrophysiology. *Behavioural Brain Research, 71,* 113–123.
Marr, D. (1982). *Vision: A computational investigation into the human representation and processing of visual information*. San Francisco: W.H. Freeman.
Martinovic, J., Gruber, T., & Müller, M. M. (2007). Induced gamma-band responses predict recognition delays during object identification. *Journal of Cognitive Neuroscience, 19,* 921–934.
Morup, M., Hansen, L. K., Herrmann, C. S., Parnas, J., & Arnfred, S. M. (2006). Parallel factor analysis as an exploratory tool for wavelet transformed event-related EEG. *Neuroimage, 29,* 938–947.
Müller, M. M., & Gruber, T. (2001). Induced gamma-band responses in the human EEG are related to attentional information processing. *Visual Cognition, 8,* 579–592.
Müller, M. M., Gruber, T., & Keil, A. (2000). Modulation of induced gamma band activity in the human EEG by attention and visual information processing. *International Journal of Psychophysiology, 38,* 283–300.
Müller, M. M., & Keil, A. (2004). Neuronal synchronization and selective color processing in the human brain. *Journal of Cognitive Neuroscience, 16,* 503–522.
Murray, J. E., & Jones, C. (2002). Attention to local form information can prevent access to semantic information. *Quarterly Journal of Experimental Psychology, 55A,* 609–625.
Perrin, F., Pernier, J., Bertrand, O., & Echallier, J. F. (1988). Spherical splines for scalp potential and current source density mapping. *Electroencephalography and Clinical Neurophysiology, 72,* 184–187.
Peterson, M. A., & Gibson, B. S. (1993). Shape recognition contributions to figure–ground organisation in three-dimensional displays. *Cognitive Psychology, 25,* 383–429.
Peterson, M. A., & Gibson, B. S. (1994a). Must figure–ground organization precede object recognition? An assumption in peril. *Psychological Science, 5,* 253–259.
Peterson, M. A., & Gibson, B. S. (1994b). Object recognition contributions to figure–ground organization: Operations on outlines and subjective contours. *Perception & Psychophysics, 56,* 551–564.
Peterson, M. A., & Skow-Grant, E. (2003). Memory and learning in figure–ground perception. In B. Ross & D. Irwin (Eds.), *Cognitive vision: Psychology of learning and motivation* (Vol. 42, pp. 1–34). London: Academic Press.
Pins, D., Meyer, M. E., Foucher, J., Humphreys, G., & Boucart, M. (2004). Neural correlates of implicit object identification. *Neuropsychologia, 42,* 1247–1259.
Posada, A., Hugues, E., Franck, N., Vianin, P., & Kilner, J. (2003). Augmentation of induced visual gamma activity by increased task complexity. *European Journal of Neuroscience, 18,* 2351–2356.
Reynolds, J. H., & Chelazzi, L. (2004). Attentional modulation of visual processing. *Annual Review of Neuroscience, 27,* 611–647.
Rugg, M. D., Soardi, M., & Doyle, M. C. (1995). Modulation of event-related potentials by the repetition of drawings of novel objects. *Cognitive Brain Research, 3,* 17–24.
Schroeder, C. E., Mehta, A. D., & Foxe, J. J. (2001). Determinants and mechanisms of attentional modulation of neural processing. *Frontiers in Bioscience, 6,* D672–D684.

Schwartz, S., Vuilleumier, P., Hutton, C., Maravita, A., Dolan, R. J., & Driver, J. (2005). Attentional load and sensory competition in human vision: Modulation of fMRI responses by load at fixation during task-irrelevant stimulation in the peripheral visual field. *Cerebral Cortex, 15,* 770–786.

Senkowski, D., & Herrmann, C. S. (2002). Effects of task difficulty on evoked gamma activity and ERPs in a visual discrimination task. *Clinical Neurophysiology, 113,* 1742–1753.

Tallon-Baudry, C., & Bertrand, O. (1999). Oscillatory gamma activity in humans and its role in object representation. *Trends in Cognitive Sciences, 3,* 151–162.

Tallon-Baudry, C., Bertrand, O., Delpuech, C., & Pernier, J. (1996). Stimulus specificity of phase-locked and non-phase-locked 40 Hz visual response in human. *European Journal of Neuroscience, 16,* 4240–4249.

Tallon-Baudry, C., Bertrand, O., Delpuech, C., & Pernier, J. (1997). Oscillatory gamma-band (30–70 Hz) activity induced by a visual search task in humans. *Journal of Neuroscience, 17,* 722–734.

Thoma, V., Hummel, J. E., & Davidoff, J. (2004). Evidence for holistic representations of ignored images and analytic representations of attended images. *Journal of Experimental Psychology: Human Perception and Performance, 30,* 257–267.

Treisman, A. M. (1969). Strategies and models of selective attention. *Psychological Review, 76,* 282–299.

Vidal, J. R., Chaumon, M., O'Regan, K. J., & Tallon-Baudry, C. (2006). Visual grouping and the focusing of attention induce gamma-band oscillations at different frequencies in human magnetoencephalogram signals. *Journal of Cognitive Neuroscience, 18,* 1850–1862.